PFC/JA-84-43

The Design of Megawatt Gyrotrons

K.E. Kreischer, B.G. Danly, J.B. Schutkeker,
and R.J. Temkin

Plasma Fusion Center
Massachusetts Institute of Technology
Cambridge, MA 02139

December 1984

This work was supported by the U.S. Department of Energy Contract No. DE-AC02-78ET51013.

The Design of Megawatt Gyrotrons

K.E. Kreischer, B.G. Danly, J.B. Schutkeker,

and R.J. Temkin

Plasma Fusion Center

Massachusetts Institute of Technology

Cambridge, MA 02139

December 1984

ABSTRACT

The design parameters of a 120 GHz gyromonotron capable of output powers in excess of 1 MW are determined. A nonlinear model of the interaction between the beam and rf field is used in which the efficiency is a function of only three normalized variables. By expressing the technological constraints in terms of these variables, permissable design parameters yielding high efficiency operation can be calculated. Constraints that are considered include ohmic heating of the walls, voltage depression of the beam, reduced coupling between the beam and rf field due to beam thickness, and efficiency degradation due to space charge forces within the beam. An analysis of the tradeoffs between current and voltage at the 1 MW level indicates that lower order modes can be utilized at lower voltages, but the constraints based on current limitations are difficult to satisfy. An 80 kV, 29 A design is presented that achieves a total efficiency of 44%. The primary uncertainty of these designs is the severity of competition due to parasitic modes. However, a number of isolated asymmetric modes appear capable of single mode emission at 1 MW based on present experimental results. Multimegawatt operation is also considered. It is shown that powers exceeding 20 MW are possible if single mode operation can be achieved in very high order modes. The methodology presented in this paper is general and can be easily adapted to other frequencies and output powers.

I. INTRODUCTION

Significant progress has been made over the past decade in the development of high power gyrotrons that can be used for electron cyclotron resonance heating (ECRH) of fusion experiments. Earlier results include cw devices that have generated powers ranging from 200 kw at 28 GHz [1] to 22 kW at 150 GHz [2]. More recently, 200 kW cw has been produced at 60 GHz [3], and long pulse gyrotrons operating at 84 GHz have generated comparable powers [4]. In addition, short pulse gyrotrons have produced powers in excess of 100 kW at 35 GHz [5], 45 GHz, 100 GHz [2], and 140 GHz [6].

The viability of using gyrotrons for ECRH has been demonstrated in a wide variety of experiments, including recent work in the United States [7,8] and the Soviet Union [9]. These experiments have shown that the efficiency of coupling the rf power to the plasma is comparable to that of other heating techiniques. As a result, gyrotrons are an attractive technology for bulk heating of fusion plasmas. One of the main advantages is the ability to place the gyrotrons well away from the containment vessel, and therefore not subject them to the harsh conditions that exist near the plasma. Other advantages include high intensity power transmission, localized heating of the plasma, and simple launcher structures. For these reasons, ECRH is a promising technique for heating fusion plasmas.

As fusion devices become larger and operate at higher magnetic fields, it will be necessary to develop cw gyrotrons that operate at both higher frequencies and at higher powers. Studies [10,11] indicate that frequencies in excess of 100 GHz will be required to heat plasmas confined by magnetic fields in excess of 3.5 T. These studies also conclude that 50 to 100 MW of rf power will be required if ECRH is to be used for bulk heating. This suggests that individual gyrotrons that generate at least 1 MW of rf power each would be attractive. In this paper, the viability of building megawatt gyrotrons at frequencies above 100 GHz will be explored.

Recent experiments that we have conducted at 140 GHz [6] indicate that efficient, single mode emission is possible at the frequencies required for ECRH. Total efficiencies of 36% and output powers of 175 kW were obtained using a single cavity. These results were in good agreement with predictions based on nonlinear theory. These experiments indicated the desirability of operating in asymmetric modes ($TE_{m,p,1}$ with $m \neq 0$) that are isolated and therefore are less susceptible to mode competition.

The primary goal of this paper is to determined the maximum power capabilities of a cw gyrotron oscillator operating at the frequencies required for ECRH. In order to minimze the amount of recirculating power in the overall system, it will be assumed that the device must operate at high efficiency. For gyrotrons, total efficiencies exceeding 40% are usually required. Based on the success of the 140 GHz experiments, this study will analyze the single cavity gyromonotron operating in an asymmetric mode. The simplicity of this configuration, as well as the success this approach has had in a variety of experiments, makes it a promising candidate. Other configurations, such as multi-cavity gyroklystrons, could further increase both power and mode selectivity. Although these alternatives will be discussed only briefly, the design techniques that will be used to analyze the gyromonotron could certainly be used in conjunction with these other configurations.

This design study is primarily concerned with the physics of the interaction between the electron beam and rf field, and the technological constraints associated with the resonator and beam. The physics is represented by the interaction efficiency and its dependence on the device parameters. By writing the technological constraints, such as wall ohmic losses and voltage depression of the beam, in terms of these parameters, it is possible to determine permissable design parameters that lead to efficient operation. In addition to determining the maximum power capabilities of a gyromonotron, a tradeoff study between the beam current and voltage has also been conducted.

This paper is primarily concerned with the cavity region, and will not deal with

problems associated with the design of the collector, transmission system, and vacuum window. Recent advances in these areas suggest many of these problems are solvable. The window appears to be the most difficult component of the overall system, especially as the operating frequency increases. It is hoped that the use of new materials with low losses, or a totally new design, will circumvent potential difficulties.

The gyrotron model used in this paper has been kept very general in order that all possible operating conditions can be explored. As a result, this analysis is more comprehensive than past studies of cw, megawatt gyrotrons [12,13,14,15]. The axial profile of the rf field has been modelled as a Gaussian rather than the sine that is typically used. A variety of experiments have found that the more realistic Gaussian model of the field leads to a better description of the operating characteristics. The possibility of choosing design parameters other than those associated with the peak efficiency has also been considered. It has been found that high efficiency operation in a lower order mode is possible by selecting operating parameters not associated with the peak efficiency. Finally, new constraints have been explored in this paper, including those associated with beam thickness, efficiency reduction due to space charge, and mode competition.

This paper will be organized in the following manner. In Section II, the model of the gyrotron interaction used in this analysis will be presented. In addition, the technological constraints that restrict the operating parameters will be reviewed. In Section III this model will be used to design a 1 MW cw gyrotron that can be used as a source for ECRH. The possibility of building multimegawatt gyrotrons will also be explored. In Section IV the implications of mode competition and its effect on mode selection will be discussed. The conclusions of this paper will be reviewed in Section V.

II. MODEL OF THE GYROTRON

In this section, the model used in this study to describe the interaction between the beam and rf field, and the technological constraints that limit the choice of design parameters, will be described. The total efficiency of the gyrotron interaction can be written as $\eta_T = \eta_\perp \eta_{el} \eta_Q$, where $\eta_\perp$ is the efficiency of energy extraction from the perpendicular component of the beam, η_{el} is the amount of beam power in the perpendicular component, and η_Q is the reduction in efficiency due to ohmic losses in the cavity walls. If $\beta_\perp = v_\perp/c$, where $v_\perp$ is the perpendicular velocity of the electrons, and $\gamma = 1 + V_c/511$, where V_c is the cathode voltage in kV, then $\eta_{el} = 0.5\beta_\perp^2/(1-\gamma^{-1})$. In order to achieve the highest efficiencies, an electron beam with the highest $\beta_\perp$ possible without mirroring is desirable. The reduction in efficiency due to cavity wall losses can be shown to be quite small in megawatt gyrotrons if the ohmic power density is restricted to a few kW/cm^2. For example, the designs described in the next section, which have wall losses limited to 2 kW/cm^2, have total ohmic losses of less than 1.7% of the output power. In this study, η_Q has been set to one.

The dependence of the total efficiency on the design parameters is primarily due to the dependence of $\eta_\perp$ on these parameters. A slow time scale analysis of the nonlinear interaction between the beam and rf field [16,17] indicates that for a given field profile, $\eta_\perp$ depends only on the following three parameters:

$$\begin{aligned} \mu &\equiv \pi \left(\frac{\beta_\perp^2}{\beta_\parallel}\right)\left(\frac{L}{\lambda}\right) \\ \Delta &\equiv \frac{2}{\beta_\perp^2}\left(1 - \frac{n\omega_c}{\omega}\right) \\ F &\equiv \frac{E_0 \beta_\perp^{n-4}}{B_0 c}\left(\frac{n^{n-1}}{2^{n-1}n!}\right) J_{m\pm n}(k_\perp R_e) \end{aligned} \tag{1}$$

In these equations $\beta_\parallel = v_\parallel/c$, where $v_\parallel$ is the parallel electron velocity, λ is the wavelength, and n is the harmonic number. The rf axial field profile is assumed to be a Gaussian of

the form $exp[-(2z/L)^2]$ extending from $-\sqrt{3}L/2$ to $\sqrt{3}L/2$. The parameter Δ indicates the detuning between the cyclotron frequency ω_c and the oscillation frequency ω. The coupling strength between the beam and rf field is represented by the parameter F, which is written in MKS units (all variables will be in MKS units unless otherwise noted). The Bessel function $J_{m\pm n}$ is a measure of the harmonic content of the rf field at the beam radius R_e. The choice of signs in the subscript depends on the direction of azimuthal rotation of the mode. The magnetic field is given by B_o, and $k_\perp = \nu_{mp}/R_o$, where R_o is the cavity radius, and ν_{mp} is the pth zero of $J'_m = 0$ and describes the transverse structure of the rf field. The definitions in (1) are based on an rf electric field in the cavity with an azimuthal component given by

$$E_\theta = RE\left[E_0 J'_m(k_\perp r)e^{(-2z/L)^2}e^{\imath(\omega t - m\theta)}\right] . \tag{2}$$

where E_0 is the amplitude.

A plot of the dependence of $\eta_\perp$ on F and μ is shown in Fig. 1 for the fundamental (n=1) interaction and the Gaussian profile given above. For each value of F and μ, the optimum Δ has been chosen such that the maximum efficiency is achieved. The shape of the isoefficeiency curves can be qualitatively understood by analyzing how the rf field amplitude and interaction length affect the work done on the electron bunch. If F and μ are small, then little work is done on the electrons and $\eta_\perp$ is small. The efficiency can be raised by increasing either of these two parameters. At some point the maximum energy extraction is achieved, and a further increase in F or μ allows the electrons to regain energy from the field and reduce the efficiency. Notice that this plot is quite general, and applies to all frequencies and powers. For example, this plot has been used as an aid to design our 100 kW experiments [6] as well as a 10 kW diagnostic gyrotron that will operate at 137 GHz on the TARA experiment [18].

In order to select a design point on Fig. 1, the various constraints that determine what

values of F and μ are acceptable must be expressed in terms of these parameters. The major constraint for cw gyrotrons is the average ohmic heating density of the resonator walls ρ_{ohm}. This is calculated by integrating the rf power flow into the cavity walls, and dividing by the surface area. If L is used as the cavity length, then ρ_{ohm} can be expressed as

$$\rho_{ohm} = 5.10 \times 10^{-15} \sigma^{-0.5} \omega^{2.5} F^2 \beta_\perp^6 C_{mp}^2 \gamma^2 \tag{3}$$

where σ is the electrical conductivity of the cavity wall, and $C_{mp} = J_m(\nu_{mp})/J_{m\pm1}(k_\perp R_e)$. In this study, $\sigma = 3.6 \times 10^7 (\Omega m)^{-1}$ has been assumed, which corresponds to annealed OFHC copper at 200°C. It should be noted that this is a representative wall temperature, and that the actual temperature will depend in a complicated manner on the design of the cooling channels and the coolant flow rate. Also note that by changing σ, a direct comparison can be made with other design studies. For example, ρ_{ohm}=2 kW/cm^2 at 200°C leads to the same design parameters based on (3) as 1.6 kW/cm^2 at room temperature.

Equation (3) shows the strong tradeoff between frequency and field amplitude, with high ω operation setting a strong upper limit on F. The mode dependence is contained in the factor C_{mp}. This variable is strongly dependent on the mode selected when operating in a lower order mode and locating the beam on an inner radial maximum of the rf field. As higher order modes are utilized and the beam is placed near the wall, this parameter approaches one and is weakly influenced by the choice of modes. For example, for potential operating modes with ν_{mp} between 15 and 22, $C_{mp} = 0.82 \pm 0.10$ for the beam located on a field maximum near the wall. In these cases, the ohmic constraint is relatively independent of the operating mode. Figure 2 shows F as a function of cathode voltage and ρ_{ohm} for 120 GHz, $\alpha = 2$, and C_{mp}=0.75. Operation at higher values of F requires either a lower voltage or an increase in the amount of power that can be dissipated in the cavity walls. For ρ_{ohm}=2 kW/cm^2, the maximum efficiency at F=0.14 would require a

relatively low voltage of 57 kV. Higher voltage operation would be possible by operating at a lower efficiency. Although this graph suggests that low voltage operation is advantageous, constraints associated with large beam currents tend to offset this result.

The next important constraint is associated with the diffractive Q, Q_D, and describes the energy balance within the cavity. The diffractive Q can be defined as $Q_D = \omega E_s/P$, where E_s is the stored energy in the resonator. For a cylindrical cavity with a Gaussian axial rf field profile, $E_s = \epsilon_o E_o^2(\pi/2)^{1.5}(L/2k_\perp^2)(\nu_{mp}^2 - m^2)J_m^2(\nu_{mp})$. In addition, previous analyses [19,20] of gyrotron cavities in which the power is extracted from the end of the resonator, as opposed to the sides, have shown that

$$Q_D = \frac{4\pi}{(1-R_2)}\left(\frac{L}{\lambda}\right)^2 \tag{4}$$

where R_2 is the reflectivity at the output end of the cavity, and the input end is assumed to have a reflectivity of one. Combining $Q_D = \omega E_s/P$ with (4), and rewriting the resulting equation in terms of F, Δ, and μ yields

$$\mu = \frac{2155F^2(1-0.5\Delta\beta_\perp^2)^2}{C_D}$$
$$where \;\; C_D = \frac{2P(MW)}{C_{mp}^2(\nu_{mp}^2 - m^2)\beta_\perp^7\gamma^2\alpha(1-R_2)} \tag{5}$$

and $\alpha = \beta_\perp/\beta_{||}$. In Fig. 3 this equation has been plotted on the isoefficiency plot (Fig. 1) assuming $\Delta\beta_\perp^2 = 0.1$.

The output power and mode strongly influence the choice of F and μ as a result of (5). For example, if F is fixed by (3), then the above equation can result in a μ that is too small for efficient energy extraction if P is too large. In this case it is usually necessary to operate in a higher order mode in order to get the desired output power. The choice of mode becomes important because of the stored energy factor $(\nu_{mp}^2 - m^2)$. For a given value of ν_{mp}, symmetric modes with $m = 0$ have the most stored energy, while whispering gallery modes with $\nu_{mp} \sim m$ have the least. It is this constraint, and not the limit on

wall loading, that typically limits whispering gallery modes to lower powers. This can be seen by noting that, for a given V_c and ω, all modes require approximately the same F based on (2). If μ is then determined by $\eta_\perp$, then whispering gallery modes will yield the lowest power according to (5) because P scales as the stored energy. Also note that (5) assumes coupling from the end of the cavity, which makes Q_D a function of the cavity length. Often the selection of L that gives the best $\eta_\perp$ results in a Q_D that is too large. This in turn requires operation in a high order mode because $(\nu_{mp}^2 - m^2) \propto PQ_D$. If Q_D were decoupled from μ, for example by extracting power from the side of the cavity, then this problem could be avoided.

The third major constraint is voltage depression of the electron beam ΔV [21,21]. This represents kinetic energy of the beam that has been transformed into potential energy and is therefore not available for conversion into rf power. In this analysis, the electrons are assumed to be uniformly distributed between cavity radii $R_e - \Delta_b/2$ and $R_e + \Delta_b/2$, where $\Delta_b = 2r_L + \Delta_g$, r_L is the Larmor radius, and Δ_g is the radial spread of the electron gyrocenters. If $\Delta_b \ll R_e$, as is typically true for a gyrotron, then

$$\Delta V = \frac{30IG(R_e, \Delta_b)}{\beta_\parallel}$$
$$where \;\; G(R_e, \Delta_b) \simeq 0.75\left(\frac{\Delta_b}{R_e}\right) + 2\ln\left(\frac{R_o}{R_e + \Delta_b/2}\right) \tag{6}$$

This beam depression consists of two components, the voltage drop from R_e to the outer edge of the beam, which is given by the first term of G, and the drop from the beam edge to the cavity wall, given by the second term. If ΔV is restricted to 10% of V_c, then an upper limit can be placed on the current, which for a given power determines the following limit on η_T:

$$\eta_T \geq \frac{1.28 \times 10^{-3} G(R_e, \Delta_b) P(MW)}{\beta_\parallel (\gamma - 1)^2} \tag{7}$$

This constraint can be made less severe by placing the beam as close to the cavity wall as possible. In this study we have restricted $R_e/R_o \leq 0.9$ in order to avoid beam interception

on the cavity wall.

There are changes in the velocity components of the beam as a result of the transformation of kinetic to potential energy. These changes can be calculated by noting that $\gamma\beta_\perp$ is a constant of the motion of the beam without the rf field present [21]. If the decrease in γ is relatively small, then most of the kinetic energy is lost from the parallel direction. This reduction in $v_{||}$ results in an upper limit on the beam current I_{MAX}. If $I = eN_e v_{||} A$, where N_e is the electron density and A is the cross-sectional area of the beam, then I_{MAX} occurs when $\partial I/\partial N_e = 0$, which gives $\partial v_{||}/\partial N_e = -v_{||}/N_e$. This leads to

$$I_{MAX} = \frac{1.71 \times 10^4 \gamma_o [1 - (1 - \beta_{||,o}^2)^{\frac{1}{3}}]^{1.5}}{G(R_e, \Delta_b)} \tag{8}$$

where γ_o and $\beta_{||,o}$ refer to these parameters without voltage depression taken into account. This constraint becomes particularly severe for low voltage operation.

The reduction in $\beta_{||}$ due to ΔV also increases the potential for beam mirroring that could ultimately disrupt the operation of the gyrotron. If $\Delta\beta_\perp/\beta_\perp$ is the perpendicular velocity spread, and no spread in γ is assumed, then the minimum $\beta_{||}$ in the beam is

$$\beta_{||,min} = \sqrt{1 - \gamma^{-2} - (\beta_\perp + \Delta\beta_\perp)^2} \tag{9}$$

By combining the definition of γ:

$$\gamma = \frac{1}{\sqrt{1 - \beta_\perp^2 - \beta_{||}^2}} \tag{10}$$

and

$$\gamma = \gamma_o - \left(\frac{\Delta V}{5.11 \times 10^5}\right) \tag{11}$$

the following equation can be derived and solved for γ:

$$(\gamma_o - \gamma)^2(\gamma^2 - C_1) = C_2^2\gamma^2 \tag{12}$$

where $C_1 = [1 + (\gamma_o \beta_{\perp,o})^2]$ and $C_2 = 5.87 \times 10^{-5} I G(R_e, \Delta_g)$. As with I_{MAX}, the effect of ΔV on $\beta_{\|}$ can be alleviated by operating at a lower current with the beam near the wall.

There are two constraints associated with the thickness of the beam. The first results from the voltage drop across Δ_g, which implies that each electron has a different γ. This drop must be limited because it represents a spread in the detuning parameter Δ. If it becomes too large, then $\eta_\perp$ cannot be optimized for all the electrons. The voltage drop also introduces some variation in the velocity components, but this effect is usually small and can be neglected. Calculations indicate that a voltage drop across Δ_g exceeding 3 kV will reduce the efficiency by more than 10% of its optimum value. In general, the drop in 1 MW devices is typically less than 1% of V_c and thus well below 3 kV, and the reduction in η_T should therefore be small.

The second condition related to beam thickness is based on coupling between the beam and rf field, and is more restrictive. According to (1), each electron sees a different value of F which depends on the radial position of its gyrocenter. If Δ_g is large compared to the width of the rf radial maximum, then the variation of F across the beam will also be large and it will not be possible to optimize $\eta_\perp$ for all electrons. In addition, a radial spread of the electrons increases the potential for multimode operation [23]. The following constraint has been used in this analysis to ensure good coupling:

$$\frac{2\Delta_g}{\lambda} < 0.3 \tag{13}$$

This inequality limits the spread of gyrocenters to 30% of $\lambda/2$, which is the minimum radial width of an rf peak in a gyrotron cavity. As a comparison, $2\Delta_g/\lambda$ was 0.21 in our 140 GHz experiments in which single mode, high efficiency operation was achieved.

The final constraint considered in this analysis is associated with space charge effects within the beam. This effect can be analyzed by including an additional factor in the slow time scale equation of motion that models the forces due to neighboring electrons

[24]. The magnitude of these forces is determined by the factor $S \equiv 4\omega_p^2/\pi\beta_\perp^2\omega_c^2$, where $\omega_p = \sqrt{e^2 N_e/\epsilon_o m_e}$. Numerical simulations indicate that there is a degradation of $\eta_\perp$ as S increases, with $-2 < \partial\eta_\perp/\partial S < -1$ for the design parameters that are being considered in this study. Based on a reduction of $\eta_\perp$ of 0.06, an upper limit of 0.04 has been used for S. This leads to the following constraint on the beam current density J:

$$J = N_e e v_{||} \leq J_s = 1.87 \times 10^4 \beta_\perp^2 \beta_{||} \omega^2(GHz) \tag{14}$$

For $\beta_\perp$=0.4, $\beta_{||}$=0.2, and ω=120 GHz, J_s=862 A/cm^2. The 1 MW designs considered in this paper have current densities of about 360 A/cm^2, comparable to the 380 A/cm^2 found in our 140 GHz experiments. Thus, in these cases (14) is easily satisfied.

III. PARAMETRIC ANALYSIS

In this section, the isoefficiency plot and constraints outlined in Section II will be used to design a 1 MW, 120 GHz gyrotron. The values of F and μ consistent with the constraints will be calculated in order to determine the interaction efficiencies that are possible and optimize the operating characteristics of the gyrotron. The major result of choosing both a higher frequency and power than is possible with present cw gyrotrons is the necessity to operate in a higher order mode. This can be seen by combining (3) and (5), and assuming $\sigma = 3.6 \times 10^7 (\Omega m)^{-1}$, which yields

$$(\nu_{mp}^2 - m^2) = \frac{2470 \mu P(MW) \omega^{2.5}(GHz)}{\beta_\perp (1 - R_2) \rho_{ohm} \alpha (1 - 0.5 \Delta \beta_\perp^2)^2} \tag{15}$$

This equation shows the strong tradeoff between power and frequency if the same operating mode is used. If both parameters are allowed to rise, then $(\nu_{mp}^2 - m^2)$ must increase, resulting in a denser mode spectrum and an increased potential for mode competition.

The restrictions of operating space based on ρ_{ohm}, Q_D, and ΔV ((3), (5), and (6) respectively), are shown in Fig. 4. This graph assumes 1 MW, 120 GHz operation with C_{mp}=0.75, R_e/R_o=0.8, and α=2. The shaded regions represent allowable operating parameters for cathode voltages of 50 and 90 kV. The upper, horizontal boundaries are due to ρ_{ohm}, which is independent of μ. As V_c increases, the regions of highest efficiency become inaccessible, and in order to obtain adequate $\eta_\perp$ the cavity length must be increased. The lower boundaries of the two regions are given by (7) and are based on $\Delta V/V_c$=0.1. In solving (7), (11) was used to calculate γ, and $\beta_\parallel$ was determined from (10) using α=2. When calculating G, $G(R_e, \Delta_b) \simeq G(R_e, 0)$ was assumed. This can be shown to be true for Δ_b consistent with (13). Figure 4 indicates that high efficiency, 1 MW operation is possible in spite of the ΔV constraint. However, this constraint will become more restrictive if the beam is placed farther from the cavity wall, or if the power is increased to multi-megawatt levels.

The dashed curves in Fig. 4 indicate the operating mode required in order that equilibrium exist in the cavity. The ν_{mp} of symmetric modes is shown, but this can be easily scaled to assymetric modes using (5). These curves assume R_2=0 and $\Delta\beta_\perp^2$=0.1, and γ and $\beta_\perp$ have been calculated neglecting the effects of voltage depression. This graph suggests that low voltage operation is advantageous and leads to operation in lower order modes. For example, for V_c=50 kV, high $\eta_\perp$ can be obtained with ν_{mp} as low as 16, while 90 kV operation requires ν_{mp} above 20 in order to achieve comparable efficiencies. However, low voltage operation requires a thick beam and $I \sim I_{MAX}$.

It order to better understand the tradeoffs between beam current and voltage, and determine if the other constraints discussed in Section II could be satisfied, an analysis of 1 MW, 120 GHz operation was done for V_c between 50 and 90 kV. If V_c is chosen, then the major unknown parameters are the mode, current, F, and μ. The four equations used in this analysis to calculate these parameters were (3), (5), $P = \eta_\perp V_\perp I$, where $V_\perp = 0.5\beta_\perp^2/(1-\gamma^{-1})V_c$, and $\eta_\perp = 0.60$. The above equation for P is convenient to use because the parameters are weakly affected by voltage depression (*eg.*, $V_\perp \simeq V_{\perp,o}$). In this analysis, $\beta_\perp$ and $\beta_{||}$ were allowed to vary consistent with (10), (11), and α=2.

The results of this study are shown in Fig. 5 for two values of R_e/R_o. The first graph indicates that the minimum ν_{mp} gradually increases as V_c increases, and is virtually the same for $R_e/R_o = 0.7$ and 0.8. Considering only symmetric modes, a beam voltage of 60 kV yields the $TE_{0,5,1}$ as the operating mode, while 83 kV requires that the $TE_{0,6,1}$ mode be chosen. Figures 5(b) through 5(d) suggest that higher voltages may be more desirable, because the constraints based on current limitations can be more easily satisfied. In Fig. 5(b), the ratio I/I_{MAX} has been plotted. For both curves, the current is a large fraction of I_{MAX} for voltages below 60 kV. This indicates substantial voltage depression is present, which could lead to a degradation of the operating characteristics. If a low V_c is selected, then the beam must be near the wall in order that I_{MAX} be sufficiently large. This could

restrict the choice of modes, and potentially require operation in a mode with severe mode competition. The higher currents required at lower V_c also result in a thicker beam, as is shown in Fig. 5(c). In order to calculate Δ_g, a current density J of 360 A/cm^2 was assumed. This is consistent with a cathode angle of 25°, a current density at the cathode of 5 A/cm^2, and B_o/B_k=30, where B_k is the magnetic field at the cathode [25]. At lower voltages, the limit given by (13) is exceeded, indicating that in these cases there is a greater reduction in η_T due to the variation of F across the beam, as well as an increased potential for mode competition. As in Fig. 5(b), increasing R_e/R_o alleviates these problems but could restrict the choice of modes. Finally, Fig. 5(d) shows the effect of velocity spread. The minimum $\beta_{\|}$ of electrons in the beam has been calculated using (9). The curves for $R_e/R_o = 0.7$ and 0.8 are virtually identical. For $\Delta v_\perp/v_\perp = 0.05$, this parameter is positive for all voltages, indicating that no electrons are reflected. However, a larger spread could result in mirroring, especially at lower V_c. Operation at higher voltages would provide a larger margin of safety.

Table I lists the design parameters for a 1 MW, 120 GHz gyrotron with V_c=80 kV, α=2, and R_e/R_o=0.8. This is a good operating voltage because the constraints considered in this study are all easily satisfied. For example, $I \ll I_{MAX}$, and Δ_g/λ is well below the limit given by (13). Voltage depression is only 2.2% of V_c. The reduction in efficiency due to space charge should be minimal, with J_s substantially larger than the 360 A/cm^2 used in this design. One uncertainty of this design is the severity of mode competition that will be experienced due to operation in a high order mode. This potential problem will be discussed in the next section.

The model described in Section II can also be used to determine the design parameters for higher power operation. The results of such an analysis are shown in Table II. The methodology used is somewhat different from that just presented for the 1 MW gyrotron. Instead of fixing P and $\eta_\perp$, the current was set at $0.7I_{MAX}$, and $(\nu_{mp}^2 - m^2)^{0.5} = 25$ was

chosen as a representative value of the highest order mode consistent with single mode operation. As in the 1 MW analysis, the frequency was fixed at 120 GHz, C_{mp}=0.75, and R_2=0. In order to maximize I_{MAX}, R_e/R_o was increased to 0.9 from 0.8. The choice of α was somewhat complicated because of the dependence of I_{MAX} on $\beta_{\|}$. Although efficiency, and therefore power, generally increase as α increases, the corresponding reduction in $\beta_{\|}$ also reduces I_{MAX}, and the net effect could be a lower output power. It was found that for the parameters given above, these opposing trends offset one another, and the net result is a weak dependence of P on α. We have therefore chosen a high value of α of 2.5 in order to obtain high efficiency operation. For each V_c, F was chosen based on (3), and μ was then varied until (5) was satisfied. The beam parameters were determined from Eqs. (6), (10), (11), and the constant of the motion $\gamma\beta$. It was found that P increased as V_c was increased because of the strong dependence of I_{MAX} on $\beta_{\|,o}$. However, η_T decreased at the same time. Therefore, the voltage that resulted in the highest power consistent with $\eta_T \geq 0.4$ was chosen as the final design.

Three different designs are given in Table II. The first column is based on a symmetric Gaussian field profile (Fig. 1) and ρ_{ohm}=2 kW/cm^2, and can be compared directly to results in Table I. The latter two columns are based on an asymmetric Gaussian with the following profile:

$$f(z) = \begin{cases} exp\left[-\left(\frac{(A+1)z}{AL}\right)^2\right] & \text{for } z < 0 \\ exp\left[-\left(\frac{(A+1)z}{L}\right)^2\right] & \text{for } z \geq 0 \end{cases} \tag{16}$$

where A represents the amount of asymmetry. A plot of $\eta_\perp(F,\mu)$ for A=2 is shown in Fig. 6. A comparison with Fig. 1 indicates that the isoefficiency curves have shifted to lower values of F and μ, and that the 70% region has greatly expanded. This suggests that, for a given mode, this profile should result in higher powers. This is supported by a comparison of the second column with the first. The most dramatic increase in power occurs when ρ_{ohm} is allowed to increase to 4 kW/cm^2. In this case, powers in excess of 7

MW are possible. The primary reason for this increase is the ability to operate at a higher voltage, which also increases I_{MAX}, and still achieve an F and μ sufficiently large for high efficiency. The voltage depression in all three cases is relatively large, but below the 10% limit discussed in the previous section. The beam thickness was calculated assuming a cathode current density of 10 A/cm^2, which yields J=720 A/cm^2. This higher density yields Δ_g for all three designs that are close to the limit given by (13). This density is also close to J_s as given by (14), suggesting that degradation due to space charge may be present in these devices.

If no limitation is placed on ν_{mp}, then the maximum power capabilities of a gyromonotron can be determined. Using constraints based on ρ_{ohm} and Q_D, one can show that powers exceeding 20 MW are possible at 120 GHz with high efficiency. Such a device could be more attractive than present high power sources, such as neutral beams, because of its inherent efficiency and the ability to place it far from the reactor. Gyrotrons capable of such high powers are possible by increasing V_c well above 100 kV, and operating close to I_{MAX}. As V_c rises, (3) necessitates operation at low F. If the isoefficiency curves in Figs. 1 and 6 continue to trend lower as μ increases, then high η_T will be possible at small F, and P will increase indefinitely. However, if these curves become horizontal, then V_c can be determined based on the minimum F consistent with a given $\eta_\perp$. For example, if $\eta_\perp \geq 0.5$ is required, then the minimum F based on a symmetric Gaussian profile is 0.03 [17], which occurs at μ=65. For $\alpha = 2.5$ and ρ_{ohm}=2 kW/cm^2, (3) gives a V_c of 180 kV, while a current of 310 A is based on $0.7I_{MAX}$. The output power is 20.6 MW, and η_T=0.37. As would be expected from the large μ and P, ν_{mp} is substantial. According to (5), ν_{mp}=131 for m=0. Whether stable, single mode operation in such a high order mode is possible remains to be determined. New techniques resulting in effective mode discrimination will undoubtedly be required.

IV. MODE COMPETITION

As ν_{mp} of the operating mode increases, the number of potential competing modes also rises. The number of parasitic modes can be approximated by determining those with an excitation region that overlaps the operating point of the desired mode Δ_{opt}. This will encompass those modes that satisfy the condition $0 \leq \Delta_{par} \leq \Delta_{opt}$, where the subscript *par* will be used to signify parasitic oscillations. Based on (1), these modes will have frequencies within the interval $\Delta\omega_{par} = 0.5\Delta_{opt}\beta_{\perp}^2\omega$. We have found that the average number N of $TE_{m,p,1}$ modes within an interval $\Delta\omega$ is well approximated for a cylindrical cavity by the expression $N = 0.28R_c^2\omega\Delta\omega/c^2$. This leads to the following equation for the average number of parasitic modes:

$$N_{par} = 0.14\left(\nu_{mp}\beta_{\perp}\right)^2\Delta_{opt} \tag{17}$$

The strong dependence on ν_{mp} is clearly evident. Using this formula for the MIT $TE_{0,3,1}$ experiment at 140 GHz, one parasitic mode would be expected. The number of competing modes increases to four for the design presented in Table I, and for the multimegawatt designs of Table II, (17) yields eight such modes. This qualitatively indicates the increasing severity of mode competition as the output power rises. Since N_{par} represents the average number of parasitic modes, it is desirable to choose an operating mode that is isolated and thus has less than N_{par} competing modes.

Two problems arise when dealing with parasitic oscillations in a gyrotron oscillator. The first is excitation of parasitic modes before the mode of interest is initiated. This is strongly dependent upon the time evolution of the voltages and current during the startup phase of operation. Parasitic modes with frequencies slightly above that of the desired mode are the most problematic. Analysis using linear theory [10] indicates that keeping V_c relatively constant during the startup phase, and therefore minimizing the variation

of Δ during this phase, reduces the potential for exciting these modes. Thus, initiating operation via anode voltage modulation is desirable. In addition to the startup phase, placement of the beam is also critical. By maximizing coupling to the mode of interest and therefore reducing its starting current, this mode can be excited at a lower current than competing ones. In some cases it may advantageous to place the beam slightly off the radial peak of the rf field in order to reduce coupling to parasitic modes to a minimum. The effectiveness of beam placement is reduced as Δ_g increases. However, if (13) is satisfied, this technique should be effective. For example, the MIT 140 GHz experiment [6] was designed with $\Delta_g/\lambda = 0.10$, and single mode emission was achieved with high efficiency in the mode of interest.

The second problem associated with parasitic oscillations is mode stability once the desired mode is excited. This requires a nonlinear analysis of the interaction between the beam and rf field. In general, if a mode is present in the cavity it strongly perturbs the beam and increases the starting current of other modes [26,27,28]. This is especially true when the gyrotron is operating near the optimum Δ of the excited mode. Numerical simulations indicate that the degree of suppression is effected not only by Δ but also by the parameter $\hat{q}$, which is a ratio of the coupling between the parasitic mode and rf field to the coupling between the operating mode and field. If $Q_{T,op} \simeq Q_{T,par}$, $\omega_{op} \simeq \omega_{par}$, and a beam with no thickness is assumed, then

$$\hat{q} = \frac{[C_{mp}^2(\nu_{mp}^2 - m^2)]_{op}}{[C_{mp}^2(\nu_{mp}^2 - m^2)]_{par}} \tag{18}$$

where the subscript *op* refers to the operating mode. The smaller $\hat{q}$ is, the harder it is to excite the parasitic mode. For example, for parameters similar to those given in Table I ($\mu_{op} = \mu_{par}$ =17 and F_{op}=0.08), Zarnitsina and Nusinovich [27] found that no parasitic mode could be excited for $\Delta_{op} > 0.2$ if $\hat{q}$ <1. Therefore, at the optimum Δ of 0.4, single mode operation would be expected if such a $\hat{q}$ could be obtained. Excitation of parasitic

modes was possible when $\Delta_{op} < 0.2$, possibly due to mode enhancement effects [23].

Although the above studies indicate single mode operation is possible if $\hat{q}$ is sufficiently small, they assumed an idealized beam with no thickness or velocity spread. It is likely that both of these effects will increase the potential for parasitic oscillations. At present, a stability analysis with these effects taken into account does not exist. Therefore, previous experimental results may give the best indication of the potential for single mode operation in megawatt gyrotrons. In the MIT experiment [6], single mode emission was achieved with η_T=0.36 in the $TE_{2,3,1}$ mode, which has virtually no competition. For the $TE_{0,3,1}$ mode, single mode emission was also achieved but the highest efficiency was 30%, or 81% of the efficiency without competition. In this case the parasitic mode was the $TE_{2,3,1}$ and $\Delta\omega/\omega = (\omega_{op} - \omega_{par})/\omega_{op}$ was 2.0%. Similar results were achieved at NRL [29] at 35 GHz using the $TE_{0,4,1}$ mode. In their case the $TE_{2,4,1}$, which has no competition, produced a peak η_T of 52%, while the $TE_{0,4,1}$ with $\Delta\omega/\omega$=1.2% yielded 40%. Therefore, reasonable efficiency appears feasible with mode separations as small as 1-2%. A number of isolated, asymmetric modes are available that could be used for one megawatt operation and satisfy this condition. For example, the $TE_{15,2,1}$ mode with R_e/R_o=0.7 is a good candidate. Its primary competing mode is the $TE_{11,3,1}$, and mode separation is 3.2%, which is larger than the separations in the above experiments.

V. CONCLUSIONS

In this paper, a parametric model was developed for a gyromonotron and used to design 120 GHz devices capable of output powers in excess of 1 MW. This model is based on a slow time scale description of the beam-rf field interaction. This theory shows that, for a given axial rf field profile, the efficiency is a function of three normalized parameters representing the interaction length, the field amplitude, and the magnetic field. By expressing the technological constraints of the gyrotron in terms of these variables, permissable design parameters leading to high efficiency operation can be determined. Constraints that were considered in this model include ohmic heating of the walls, the diffractive Q of the cavity, voltage depression of the beam, reduced coupling between the beam and rf field due to beam thickness, and efficiency degradation due to space charge forces within the beam. This model was kept as general as possible in order that all possible operating conditions could be explored. As a result, it can be applied to a wide range of frequencies and powers.

A 1 MW device was analyzed in order to determine the optimum cathode voltage and beam current. It was found that as the voltage increased, the ohmic heating limit required a reduction in the field amplitude, and a corresponding increase in the interaction length. This increased the cavity Q and led to operation in a higher order mode. Therefore, it is desirable to choose the lowest voltage consistent with the constraints associated with the beam current. The design parameters of an 80 kV, 29 A gyrotron with an efficiency of 44% were calculated and are given in Table I. It was also found that voltage depression becomes evident at the 1 MW level, and thus the beam parameters must be calculated consistent with this effect. This is especially true as the current approaches the upper limit given by (8). The design in Table I requires an oversized cavity with the potential for severe mode competition. However, a number of isolated asymmetric modes appear capable of single mode emission and good efficiencies based on a comparison with mode separations in present experiments.

Multimegawatt operation was also considered in this study. One set of designs was calculated based on a current of $0.7I_{MAX}$ and a mode index ν_{mp} of 25. The designs were chosen by increasing the voltage as much as possible while maintaining $\eta_T \geq 0.4$. For a wall heating of 2 kW/cm^2 and a symmetric Gaussian field profile, 3.2 MW could be generated. By using an asymmetric Gaussian, which produces higher efficiencies for a given length and rf field, powers could be increased to 4.0 MW. The biggest change occurred when the wall heating limit was increased to 4 kW/cm^2. In this case 7.3 MW was possible. If no limitation is placed on ν_{mp}, then even higher powers can be generated. For example, if $\eta_\perp \geq 0.5$ is required, then powers in excess of 20 MW are possible. Thus, the gyrotron is a source capable of producing extremely high power efficiently in the millimeter range.

In this paper, the gyrotron was modelled as a single cavity oscillator. One of the uncertainties of this configuration is the ability to achieve single mode emission. Previous experiments suggest that isolated, asymmetric modes should make this possible to the 1 MW level. Beyond this other designs, or mode selection techniques, may be required. The possibilities include multiple cavity devices such as gyroklystrons or gyrotwystrons. These sources are based on prebunching of the beam by a mode that can be controlled, which results in effective discrimination against modes at other frequencies or with different azimuthal field structures. In addition, the prebunching results in high efficiency at shorter interaction lengths and leads to operation in lower order modes. Another potential technique is injection locking by an external source. The methodology presented in this study will still be relevant for these devices if the appropriate isoefficiency graphs can be generated. Then the constraints discussed here, as well as new limitations introduced by the devices, can be used to determine optimized designs.

REFERENCES

[1] H. Jory, S. Evans, J. Moran, J. Shively, D. Stone and G. Thomas, "200 kW pulsed and CW gyrotrons at 28 GHz," in *IEDM Tech. Dig.*, 1980, paper 12.1, pp. 304-307.

[2] A. A. Andronov, V. A. Flyagin, A. V. Gaponov, A. L. Gol'denberg, M. I. Petelin, V. G. Usov and V. K. Yulpatov, "The gyrotron: High-power source of millimetre and submillimetre waves," *Infrared Phys.*, vol. 18, pp. 385-393, 1978.

[3] K. Felch, R. Bier, L. Fox, H. Huey, H. Jory, N. Lopez, J. Manca, J. Shively, and S. Spang, "Gyrotrons for plasma heating experiments," in *Proc. Fourth Int. Symp. on Heating in Toroidal Plasmas*, Rome, 1984, pp. 1165-1170.

[4] V.A. Flyagin, V.V. Alikaev, K.M. Likin, G.S. Nusinovich, V.G. Usov, and S.N. Vlasov, "A gyrotron complex for electron-cyclotron plasma heating in the T-10 Tokamak," in *Proc. Third Joint Varenna-Grenoble Int. Symp.*, 1982, pp. 1059-1065.

[5] Y. Carmel, K.R. Chu, M. Read, A.K. Ganguly, D. Dialetis, R. Seeley, J.S. Levine, and V.L. Granatstein, "Realization of a stable and highly efficient gyrotron for controlled fusion," *Phys. Rev. Lett.*, vol. 50, pp. 112-116, 1983.

[6] K.E. Kreischer, J.B. Schutkeker, B.G. Danly, W.J. Mulligan, and R.J. Temkin, "High efficiency operation of a 140 GHz pulsed gyrotron," MIT-PFC/JA-84-17, to be published in *Int. J. Electronics*, 1984.

[7] H. Hsuan, K. Bol, N. Bowen, D. Boyd, A. Cavallo, A. Dimits, J. Doane, G. Elder, M. Goldman, B. Grek, C. Hoot, D. Johnson, A. Kritz, B. Leblanc, P. Manintveld, R. Polman, S. Sesnic, H. Takashashi, and F. Tenney, "Major results of the electron cyclotron heating experiment in the PDX tokamak," *Proc. Fourth Int. Symp. on Heating in Toroidal Plasmas*, Rome, 1984, pp. 809-833.

[8] R. Prater, "High power electron cyclotron heating experiments in the Doublet III Tokamak," *Bull. Am. Phys. Soc.*, vol. 29, p. 1259, 1984.

[9] V. V. Alikaev, *et al.*, "Plasma heating in the T-10 at the second ECR harmonic," *Sov. J. Plasma Phys.*, vol. 9, pp. 196-200, 1983

[10] K.E. Kreischer, and R.J. Temkin, "High frequency gyrotrons and their applications to tokamak plasma heating", in *Infrared and Millimeter Waves*, vol. 7, New York: Academic Press, 1983, 377-485.

[11] S.M. Wolfe, D.R. Cohn, R.J. Temkin, and K. Kreischer, "Characteristics of electron-cyclotron-resonance-heated tokamak power reactors," *Nuclear Fusion*, vol. 19, pp. 389-399, 1979.

[12] K.J. Kim, M.E. Read, J.M. Baird, K.R. Chu, A. Drobot, J.L. Vomvoridis, A. Ganguly, D. Dialetis, and V. Granatstein, "Design considerations for a megawatt CW gyrotron," *Int. J. Electronics*, vol. 51, pp. 427-445., 1981.

[13] H. Jory, "Status of gyrotron developments at Varian Associates," in *Proc. Fourth Int. Symp. on Heating in Toroidal Plasmas*, Rome, 1984, pp. 1424-1430.

[14] N.J. Dionne, A. Palevsky, and R. Mallavarpu, "One megawatt, 100 GHz, gyrotron study," ORNL/Sub-83/59396/1, 1983.

[15] M.E. Read, A. Fliflet, K.J. Kim, K.R. Chu, W. Mannheimer, "Report on studies for CW megawatt gyrotrons," D.O.E. report DOE/ET/52053, 1983.

[16] G.S. Nusinovich, and R.E. Erm, "Efficiency of a CRM monotron with a Gaussian longitudinal distribution of high frequency fields," *Elektronnaya Tekhnika*, Ser. 1, Elektronika SVCh, pp. 55-60, 1972.

[17] B.G. Danly, MIT-PFC/JA-85-6, 1985.

[18] P. Woskoboinikow, D.R. Cohn, M. Gerver, W.J. Mulligan, R.S. Post, R.J. Temkin, and J. Trulsen, "A high frequency gyrotron scattering diagnostic for instability studies on TARA," MIT-PFC/JA-84-32, to be published in *Rev. Scientific Inst.*

[19] S. N. Vlasov, G. M. Zhislin, I. M. Orlova, M. I. Petelin, and G. G. Rogacheva, "Irregular waveguides as open resonators," *Radiophys. Quantum Elect.*, vol. 12, pp. 972-978, 1969.

[20] R.J. Temkin, "Analytic theory of a tapered gyrotron resonator," *Int. J. Inf. and Mm. Waves*, vol. 2, pp. 629-650, 1981.

[21] A.K. Ganguly and K.R. Chu, "Limiting Current in Gyrotrons," *Int. J. Inf. and Mm. Waves*, vol. 5, pp. 103-122, 1984.

[22] A.T. Drobot and K. Kim, "Space charge effects on the equilibrium of guided electron flow with gyromotion," *Int. J. Electronics*, vol. 51, pp. 351-367, 1981.

[23] K.E. Kreischer, R.J. Temkin, H.R. Fetterman, and W.J. Mulligan, "Multimode oscillation and mode competition in high frequency gyrotrons," *IEEE Trans. Microwave Theory Tech.*, vol. MTT-32, pp. 481-490, 1984.

[24] V.L. Bratman and M.I. Petelin, "Optimizing the parameters of high-power gyromonotrons with RF-field of non-fixed structure," *Radiophysics and Quantum Electronics*, vol. 18, pp. 1136-1140, 1975.

[25] K. Felch, D. Stone, H. Jory, R. Garcia, G. Wendell, R.J. Temkin, and K.E. Kreischer, "Design and operation of magnetron injection guns for a 140 GHz gyrotron," in IEDM Tech. Dig., 1982, paper 14.1, pp. 362-365.

[26] D. Dialetis, and K.R. Chu, "Mode competition and stability analysis of the gyrotron oscillator," in *Infrared and Millimeter Waves*, vol. 7, New York: Academic Press, 1983,

pp. 537-581.

[27] I.G. Zarnitsina and G.S. Nusinovich, "Stability of single-mode self-excited oscillations in a gyromonotron," *Radiophysics and Quantum Electronics*, vol. 17, pp. 1418-1424, 1974.

[28] G.S. Nusinovich, "The effectiveness of nonlinear mode selection methods in MCR oscillators," *Radio Engineering and Electronic Physics*, vol. 22, pp. 151-152, 1977.

[29] Y. Carmel, K.R. Chu, D. Dialetis, A. Fliflet, M. R. Read, K.J. Kim, B. Arfin, and V. L. Granatstein, "Mode competition, suppression, and efficiency enhancement in over-moded gyrotron oscillators, *International Journal of Infrared and Millimeter Waves*, vol. 3, pp. 645-665, 1982.

Parameter	Design Value
I (A)	28.7
η_T (%)	43.5
$\beta_\perp$	0.44
$\beta_\parallel$	0.22
F	0.091
μ	15.1
Minimum ν_{mp}	18.9
Δ V/V (%)	2.2
I_{MAX} (A)	115
R_e (cm)	0.60
Δ_g/λ	0.085
J_s (A/cm^2)	1190
Q_T	365
B_o (T)	4.7

Table I. Design parameters for a 1 MW, 120 GHz, gyrotron with a symmetric Gaussian axial field profile and V_c=80 kV.

Asymmetry	A=1	A=2	A=2
ρ_{ohm}(kW/cm^2)	2.0	2.0	4.0
P(MW)	3.2	4.0	7.3
I(A)	118	138	182
V_c(kV)	70	80	100
$\eta_\perp$(%)	51	48	54
η_T(%)	39	36	40
F	0.10	0.085	0.09
μ	10.0	8.5	10.1
Δ V/V(%)	6.2	6.0	5.8
Δ_g/λ	0.12	0.14	0.18

Table II. Design parameters for 120 GHz, multimegawatt gyrotrons with Gaussian axial field profiles and $(\nu_{mp}^2 - m^2)^{\frac{1}{2}}$=25.

FIGURES

Figure 1 Perpendicular efficiency $\eta_\perp$, optimized with respect to Δ, versus the normalized field amplitude F and the normalized interaction length μ. The rf field profile is a symmetric Gaussian.

Figure 2 The field amplitude F versus cathode voltage and cavity wall ohmic heating density for 120 GHz. Curves were derived from (3) assuming $\alpha \equiv \beta_\perp/\beta_{||}$=2 and C_{mp}=0.75.

Figure 3 Operating conditions based on an energy balance within the cavity superimposed on Fig. 1. C_D is defined in (5).

Figure 4 Shaded regions represent allowable operating regions for cathode voltages of 50 and 90 kV assuming 1 MW, 120 GHz operation. Dashed lines are mode indices ν_{mp} based on an equilibrium in the cavity.

Figure 5 Design parameters versus cathode voltage for 1 MW, 120 GHz operation. (a)- The minimum mode index. (b)- The ratio of beam current to the maximum current given by (8). (c)- The radial spread in gyrocenters Δ_g. (d)- The minimum $\beta_{||}$ in the beam assuming a velocity spread $\Delta v_\perp/v_\perp$ of 5%.

Figure 6 Isoefficiency plot, similar to Fig. 1, for an asymmetric Gaussian field profile with A=2 (see (16)).

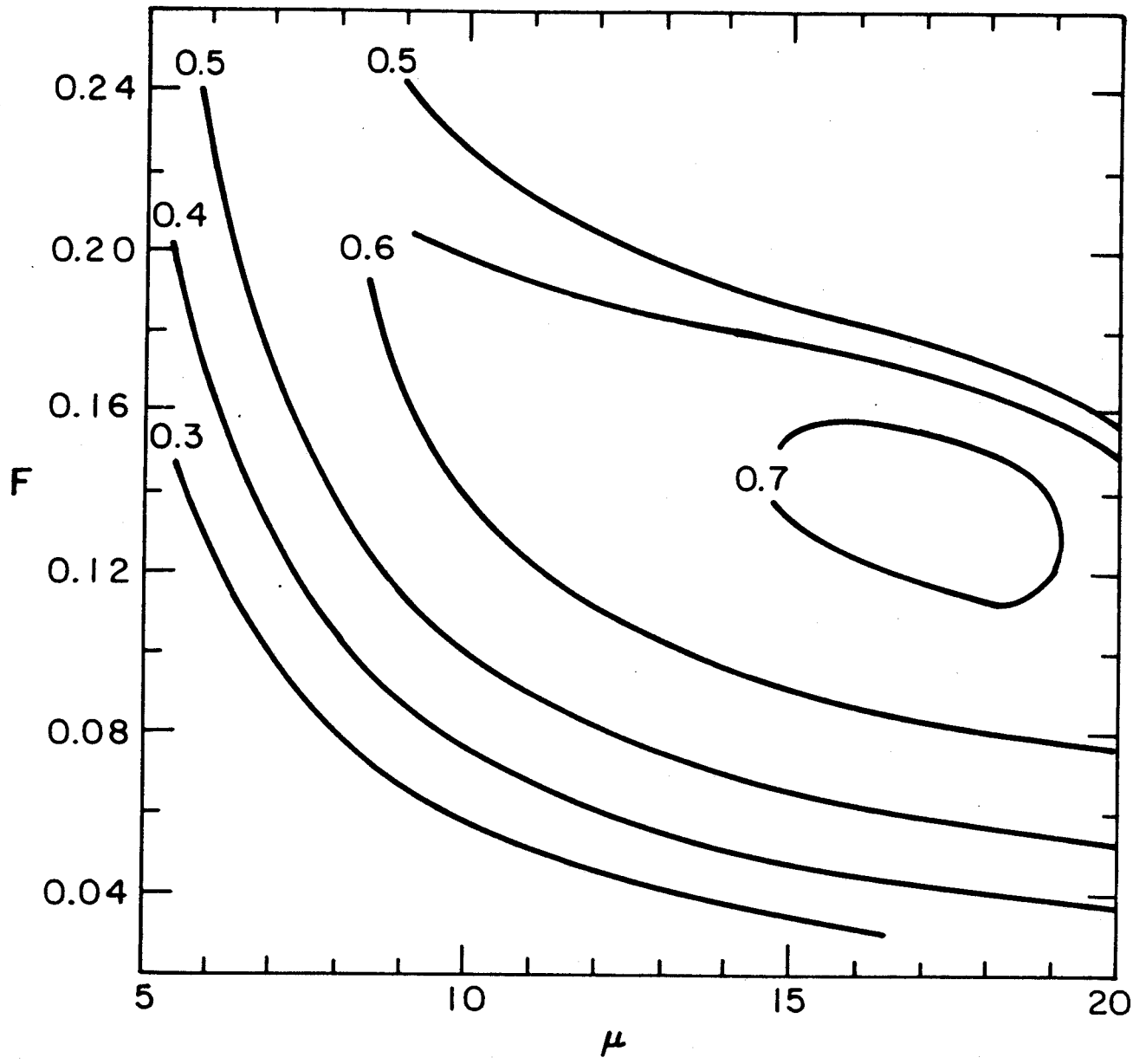

Figure 1

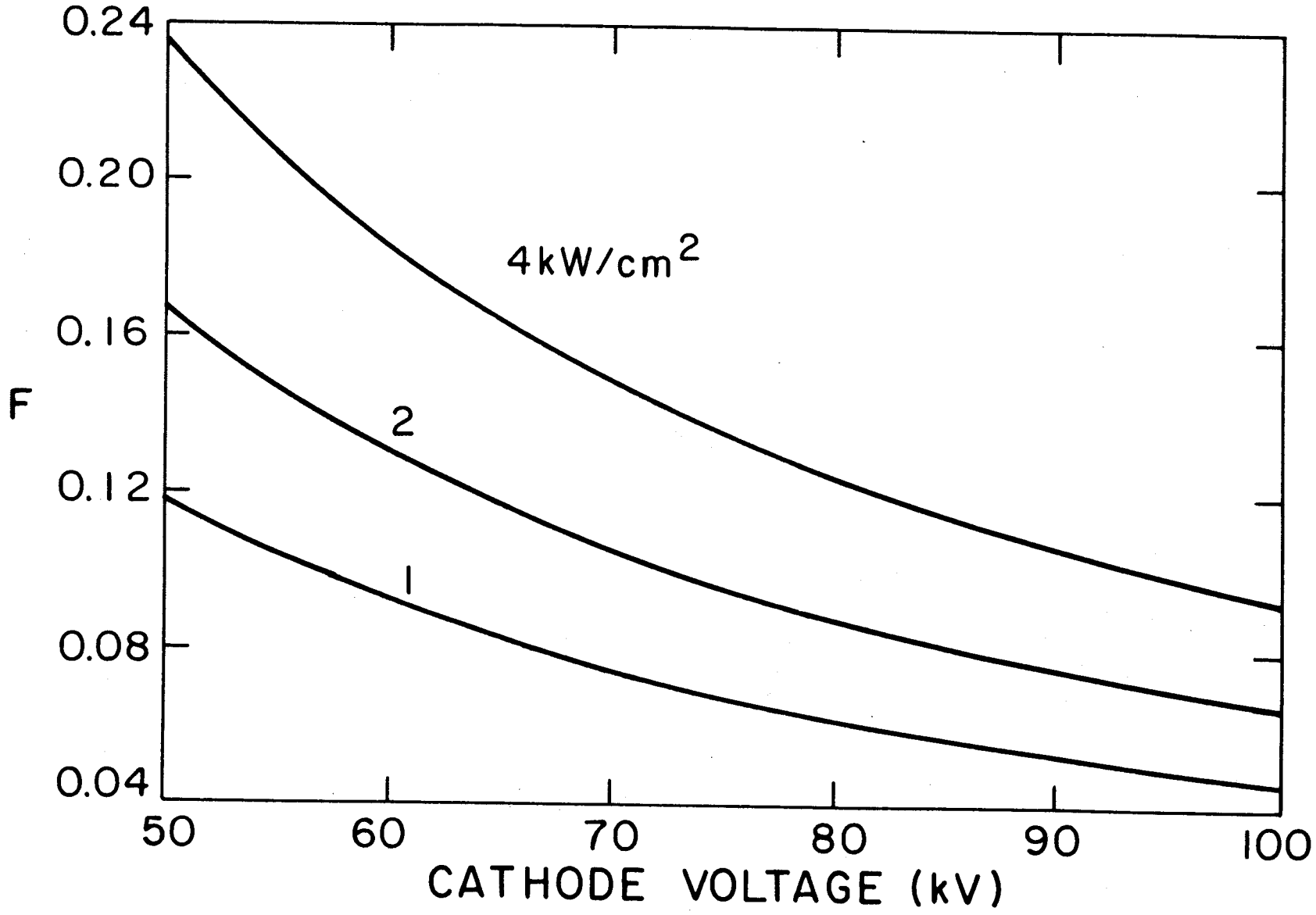
0.24
0.20
0.16
0.12
0.08
0.04
F
4kW/cm2
2
1
50
60
70
80
90
100
CATHODE VOLTAGE (kV)

Figure 2

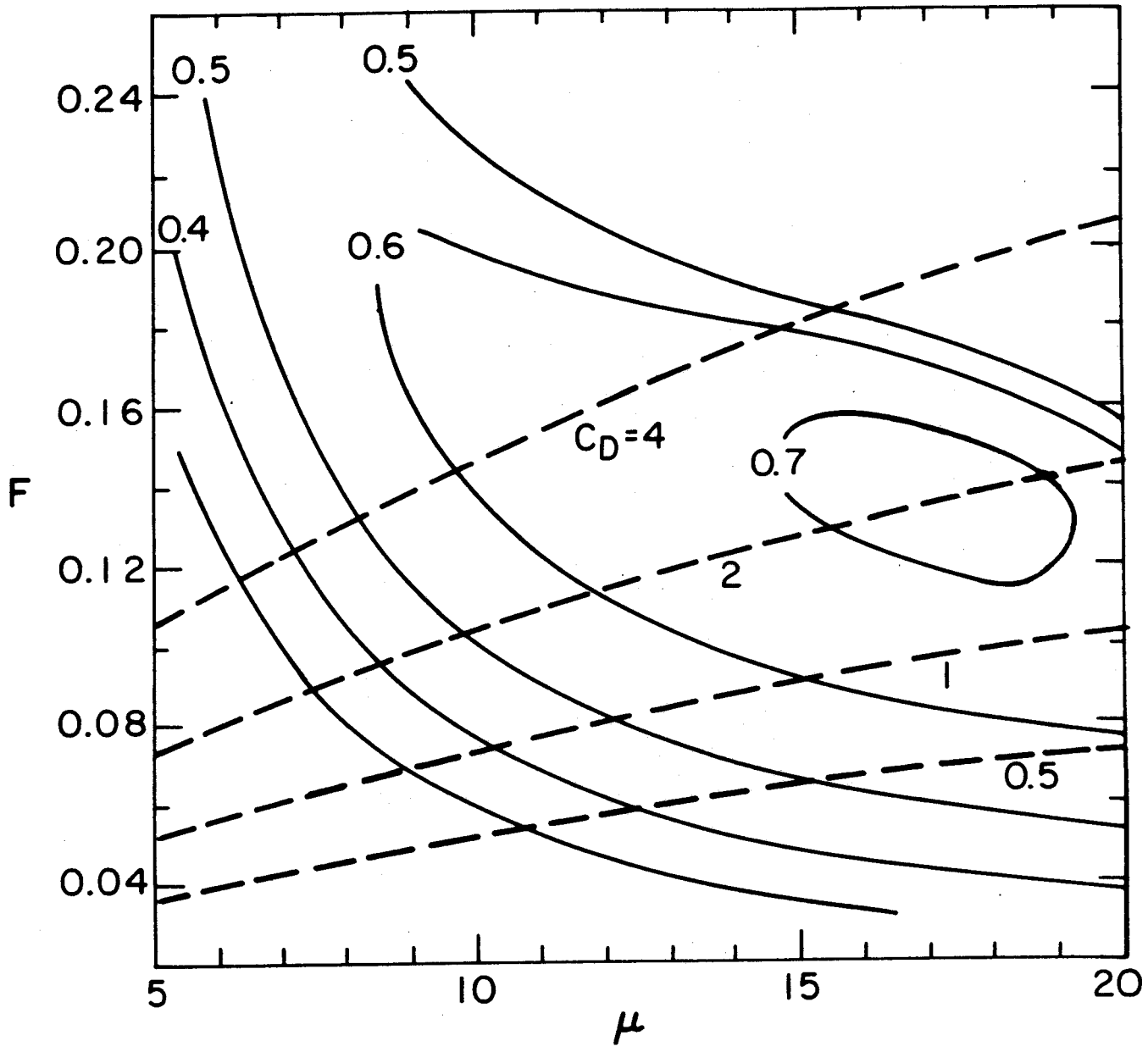

Figure 3

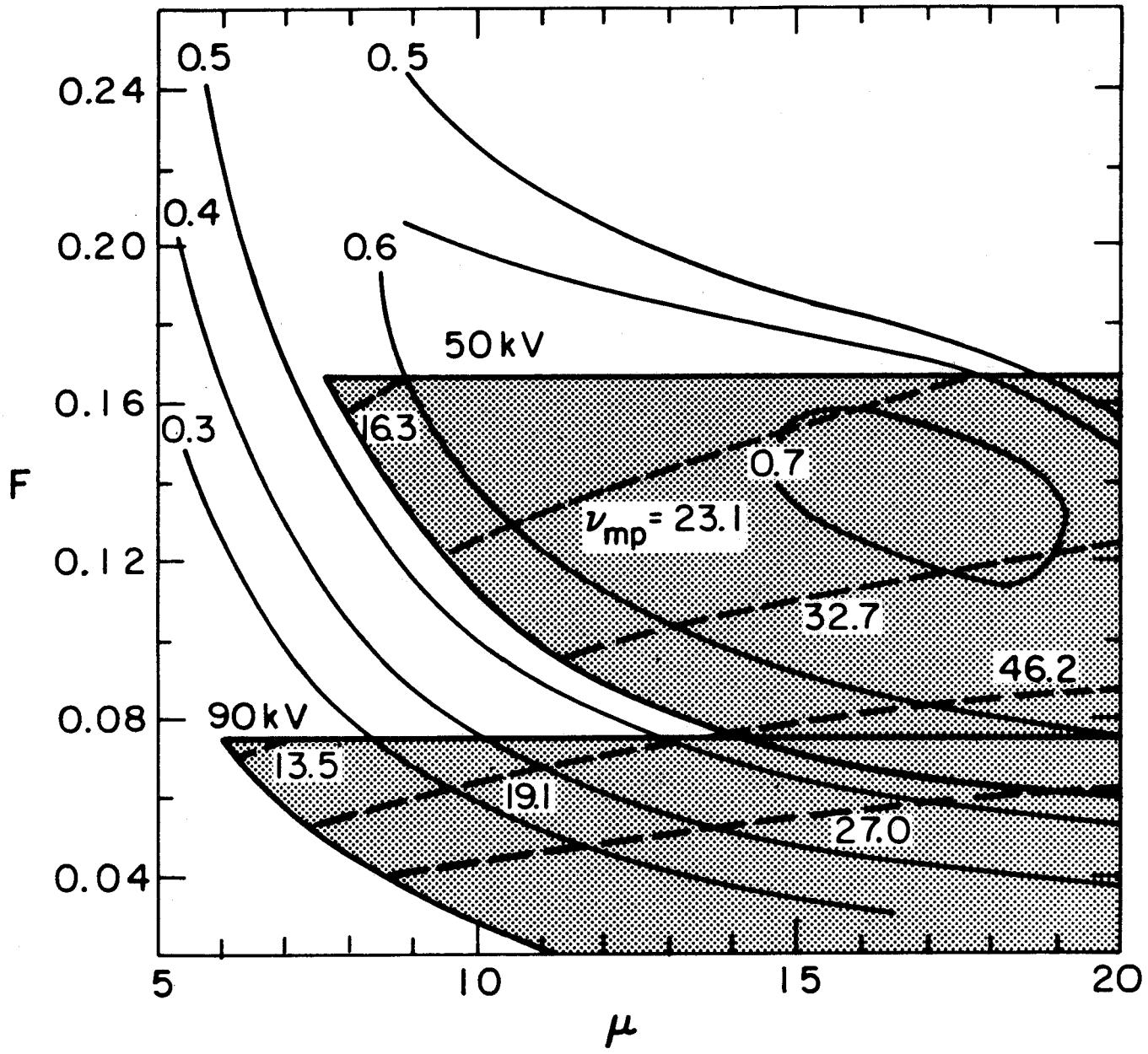
0.5
0.5
0.24
0.4
0.20
0.6
50kV
0.16
0.3
F
16.3
0.7
ν_{mp} = 23.1
0.12
32.7
46.2
0.08
90kV
13.5
19.1
27.0
0.04
5
10
15
20
μ

Figure 4

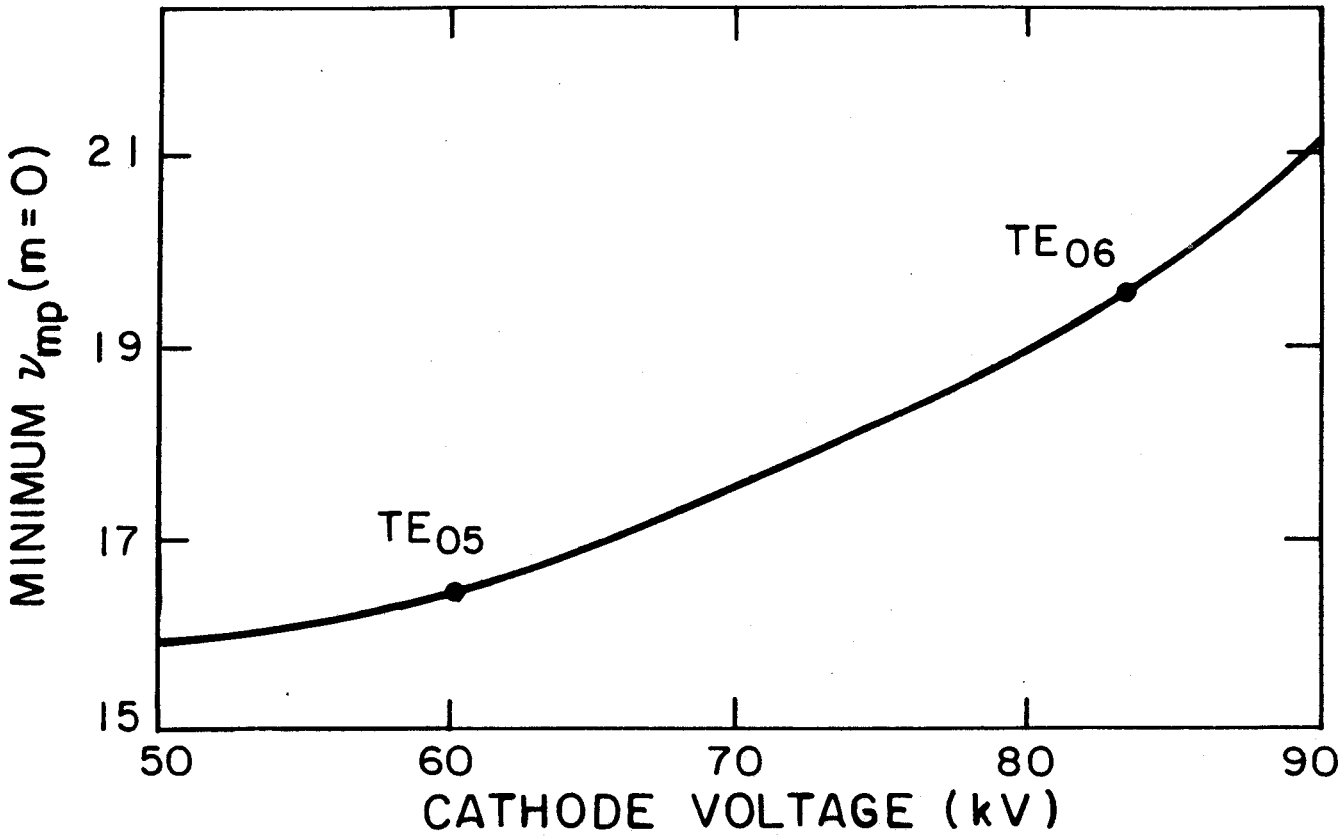

Figure 5 (a)

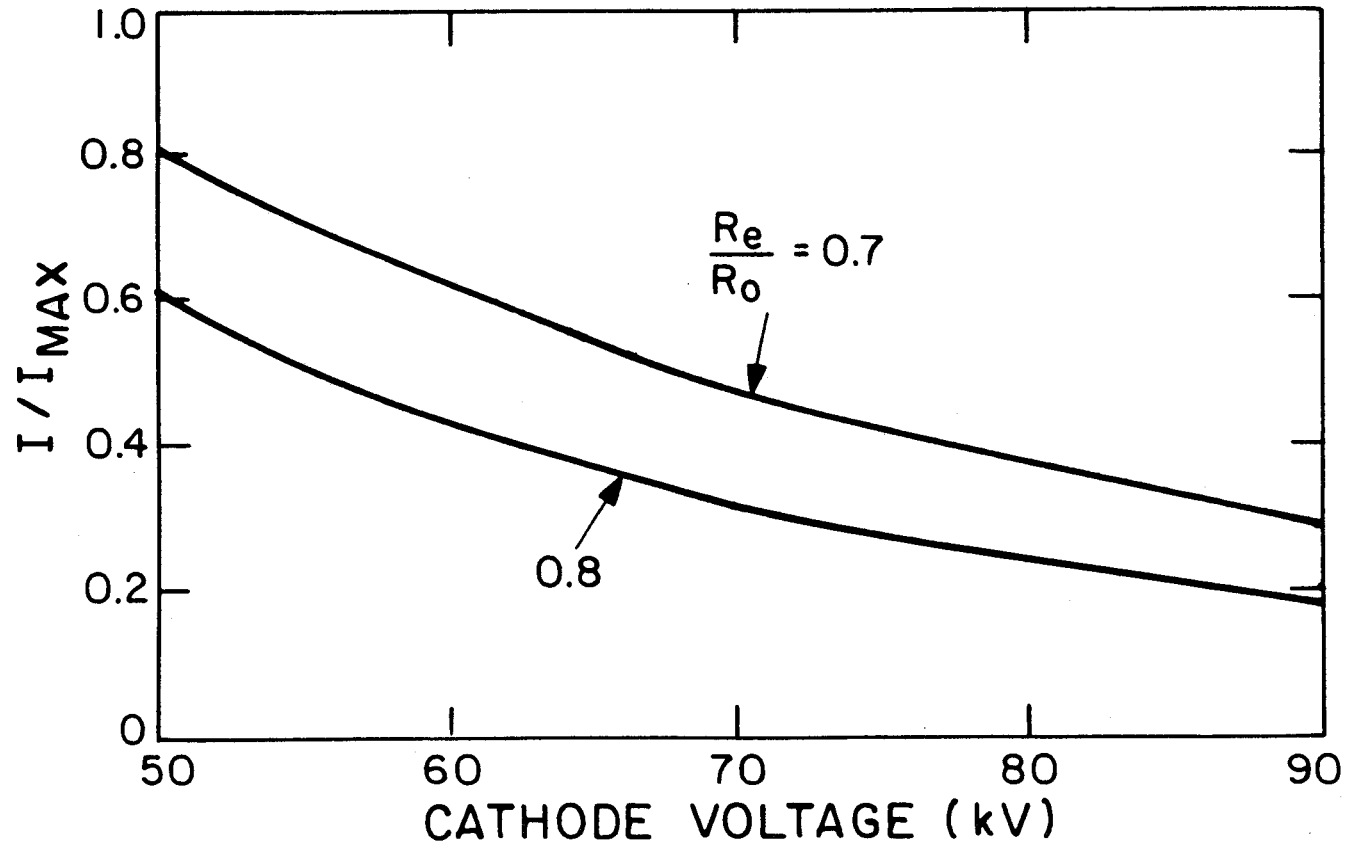

Figure 5 (b)

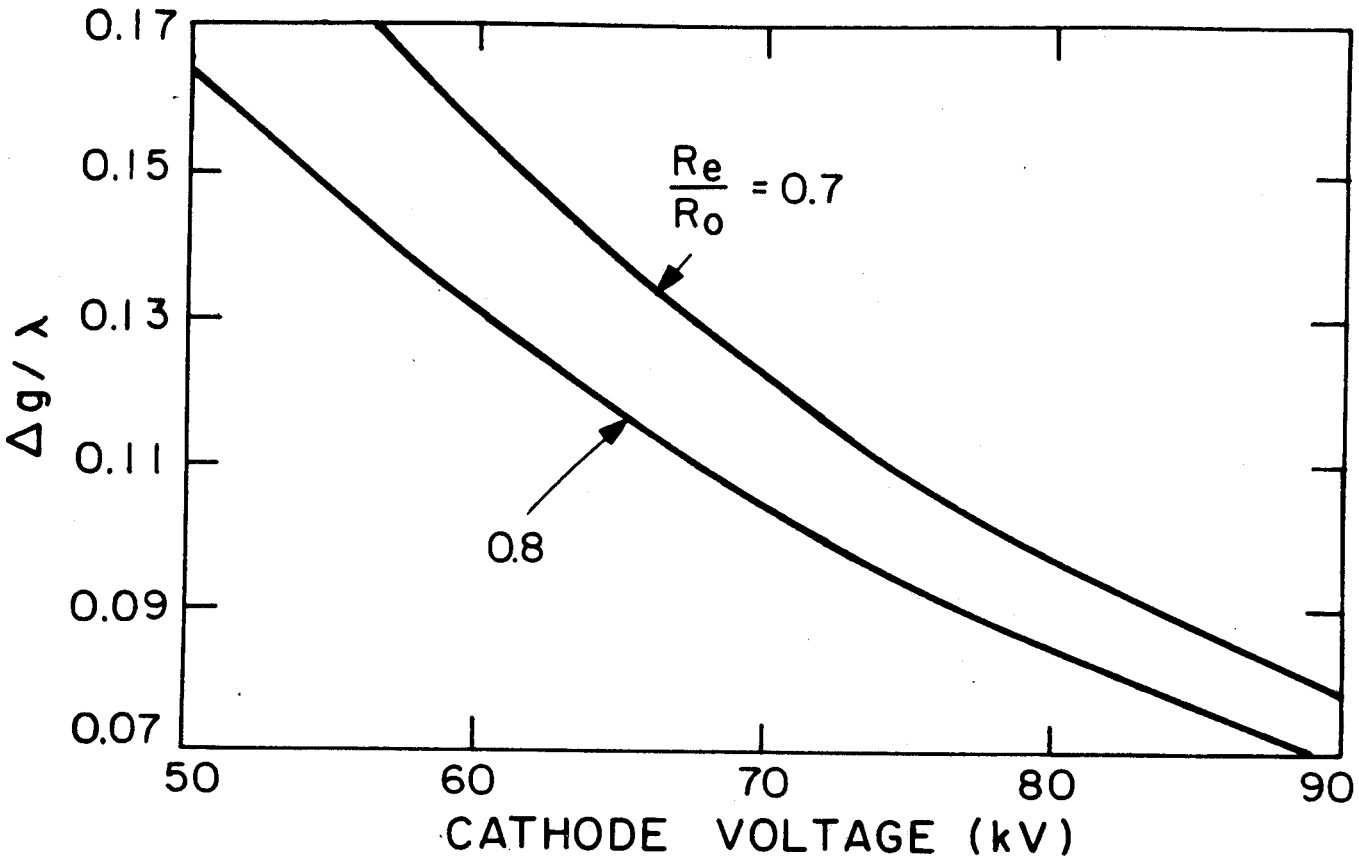

Figure 5 (c)

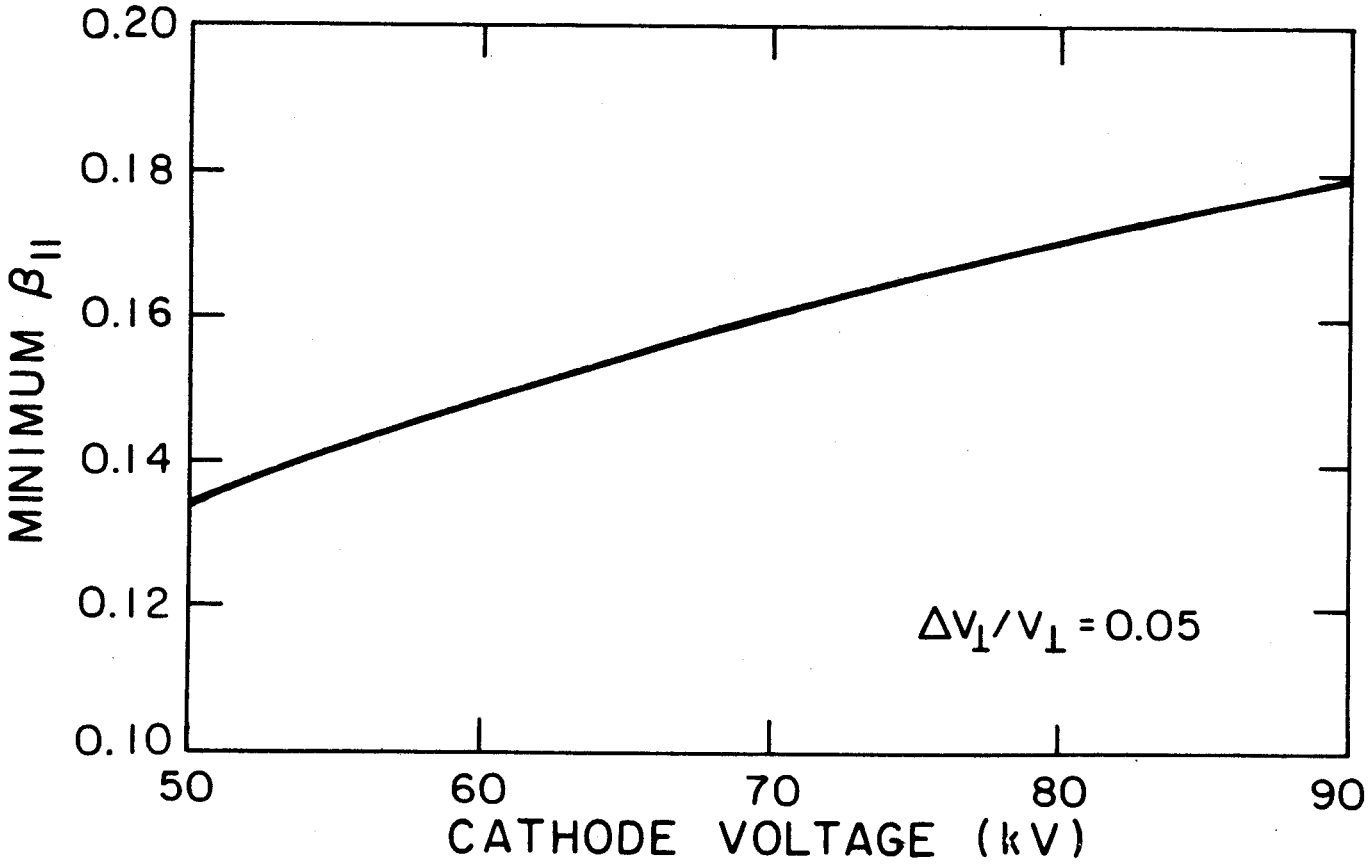

Figure 5 (d)

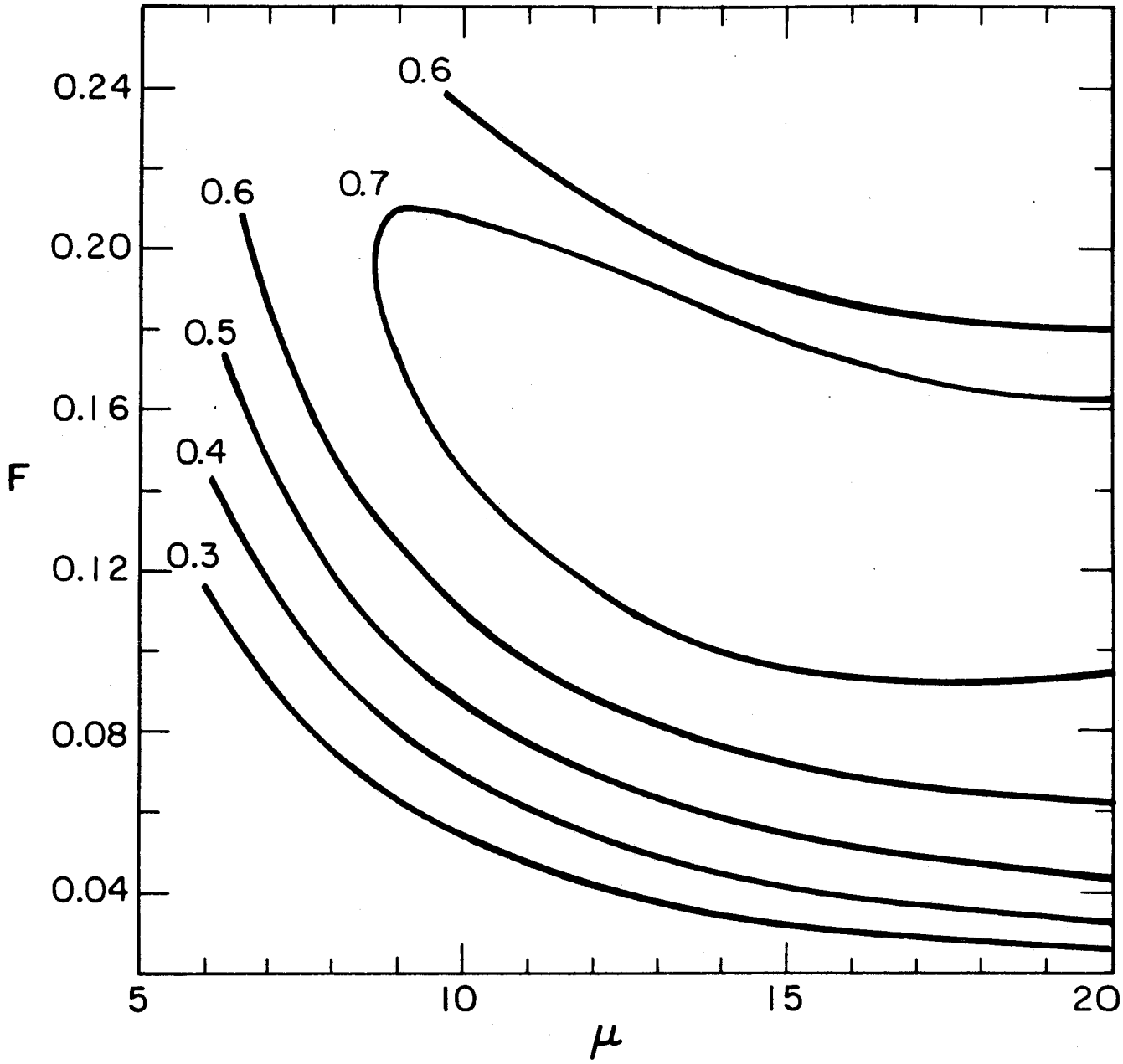

Figure 6